Loss of high-frequency glucose-induced Ca^{2+} oscillations in pancreatic islets correlates with impaired glucose tolerance in *Trpm5*$^{-/-}$ mice

Barbara Colsoul[a,1], Anica Schraenen[b,1], Katleen Lemaire[b], Roel Quintens[b], Leentje Van Lommel[b], Andrei Segal[a], Grzegorz Owsianik[a], Karel Talavera[a], Thomas Voets[a], Robert F. Margolskee[c], Zaza Kokrashvili[c], Patrick Gilon[d], Bernd Nilius[a,2], Frans C. Schuit[b,2], and Rudi Vennekens[a,2,3]

[a]Laboratory of Ion Channel Research and [b]Gene Expression Unit, Department of Molecular Cell Biology, Katholieke Universiteit Leuven, B-3001 Louvain, Belgium; [c]Department of Neuroscience, Mount Sinai School of Medicine, New York, NY 10029; and [d]Unit of Endocrinology and Metabolism, Faculty of Medicine, University of Louvain, B-1000 Brussels, Belgium

Edited* by Lutz Birnbaumer, National Institute of Environmental Health Sciences, Research Triangle Park, NC, and approved February 1, 2010 (received for review November 12, 2009)

Glucose homeostasis is critically dependent on insulin release from pancreatic β-cells, which is strictly regulated by glucose-induced oscillations in membrane potential (V_m) and the cytosolic calcium level ($[Ca^{2+}]_{cyt}$). We propose that TRPM5, a Ca^{2+}-activated monovalent cation channel, is a positive regulator of glucose-induced insulin release. Immunofluorescence revealed expression of TRPM5 in pancreatic islets. A Ca^{2+}-activated nonselective cation current with TRPM5-like properties is significantly reduced in *Trpm5*$^{-/-}$ cells. Ca^{2+}-imaging and electrophysiological analysis show that glucose-induced oscillations of V_m and $[Ca^{2+}]_{cyt}$ have on average a reduced frequency in *Trpm5*$^{-/-}$ islets, specifically due to a lack of fast oscillations. As a consequence, glucose-induced insulin release from *Trpm5*$^{-/-}$ pancreatic islets is significantly reduced, resulting in an impaired glucose tolerance in *Trpm5*$^{-/-}$ mice.

Ca^{2+} signaling | insulin release | pancreatic β-cells | transient receptor potential ion channels | glucose sensing

The pancreatic β-cell is an electrically excitable cell that secretes insulin when extracellular glucose levels exceed a threshold concentration. Characteristically, upon stimulation with glucose, β-cells display an oscillatory change of the membrane potential (V_m) and, in parallel, of the cytosolic Ca^{2+} level ($[Ca^{2+}]_{cyt}$) (1–4). This pattern, consisting of slow waves of depolarized plateaus on which bursts of action potentials are superimposed and separated by electrically silent intervals, plays a critical role in the regulation of insulin secretion. Indeed, in the absence of depolarization, no insulin is released, and the "extent" of electrical activity largely determines the amount of released insulin (1, 5). The bursting pattern of the β-cell is a complex interplay among different ion channels (e.g., ATP-sensitive K^+ channels, voltage-gated Ca^{2+} channels, and Ca^{2+} and voltage-activated K^+ channels), intracellular Ca^{2+} levels ($[Ca^{2+}]_{cyt}$), and the cellular metabolism of the β-cell (1, 6). The increase in $[Ca^{2+}]_{cyt}$ originates from glucose-induced Ca^{2+} influx through voltage-gated L-type Ca^{2+} channels and, possibly, Ca^{2+} mobilization from intracellular stores, the latter promoted by activation of the phospholipase C system and generation of inositol 1,4,5-trisphosphate (1, 7, 8). Despite intensive investigation, several aspects of the rhythmic electrical activity of β-cells, such as the origin of the variability in oscillation pattern, remain unclear. Indeed, glucose stimulation can result in high-frequency short bursts, low-frequency long bursts, or a combination of these two patterns, also known as compound bursts (9, 10).

In this study we identified TRPM5 as a player in the electrical activity of glucose-stimulated pancreatic β-cells. TRPM5 is one of 28 members of the large transient receptor potential (TRP) superfamily (11–13). TRPM5, and its close homologue TRPM4, are Ca^{2+}-activated cation channels that are permeable for monovalent cations, but not divalent cations, with a conductance of approximately 20 to 25 pS (14–16). Using *Trpm5*$^{-/-}$ mice we show here that this channel promotes high-frequency glucose-induced oscillations in V_m and $[Ca^{2+}]_{cyt}$ in pancreatic β-cells. Loss of TRPM5 expression, and high-frequency bursting, is functionally relevant as this leads to reduced glucose-induced insulin release from isolated islets and impaired glucose tolerance.

Results and Discussion

Expression of the *Trpm5* Gene in Pancreatic β-Cells. Previously, *Trpm5* expression was shown on the mRNA level in several β-cell lines and in human and mouse tissues, including taste buds, intestine, and pancreatic islets (13, 17–22). Here we describe immunostaining of TRPM5 protein in pancreatic islets with a specific antibody (Fig. 1). TRPM5 is colocalized with insulin in WT islets, strongly suggesting expression of TRPM5 in insulin secreting β-cells. Specific staining with the TRPM5 antibody is absent in *Trpm5*$^{-/-}$ islets. Quantitative PCR experiments in a purified β-cell sample confirmed expression of *Trpm5* in the β-cells. Expression of *Trpm5* could also be detected in purified α-cells, although to a lower level compared with β-cells (Fig. S1).

Characterization of a Ca^{2+} Release–Activated Cation Current in Pancreatic Islet Cells. To determine whether TRPM5 is part of the Ca^{2+}-activated monovalent cation current described earlier in insulin-secreting cell lines and primary β-cells (23–25), we compared whole-cell currents in WT and *Trpm5*$^{-/-}$ single pancreatic islet cells. Only cells with a cell capacitance of >5 pF were analyzed, being most likely pancreatic β-cells (26). In one approach, cells were dialyzed with a pipette solution containing 1.5 μM Ca^{2+}. As shown in Fig. 2, a Ca^{2+}-dependent cation current can be readily activated, which is largely reduced in *Trpm5*$^{-/-}$ cells (Fig. 2 *A–C*). Comparable results were obtained when $[Ca^{2+}]_{cyt}$ was increased by flash-uncaging during whole-cell experiments (WT, 6.5 ± 1.4 pA/pF; vs. *Trpm5*$^{-/-}$, 3.5 ± 0.5 pA/pF; $P = 0.035$ at –80 mV; WT, 2.53 ± 0.7 pA/pF; vs. *Trpm5*$^{-/-}$, 1.09 ± 0.2 pA/pF; $P = 0.025$ at +80 mV; n = 21–27 from five to six mice). Ca^{2+} uncaging during a step to +80 mV (Fig. 2*D*) allows

Author contributions: B.C., A. Schraenen, T.V., R.F.M., P.G., B.N., F.C.S., and R.V. designed research; B.C., A. Schraenen, K.L., R.Q., A. Segal, G.O., Z.K., and R.V. performed research; B.C., A. Schraenen, L.V.L., A. Segal, G.O., K.T., T.V., R.F.M., Z.K., P.G., and R.V. contributed new reagents/analytic tools; B.C., A. Schraenen, K.L., T.V., P.G., B.N., F.C.S., and R.V. analyzed data; and B.C., A. Schraenen, B.N., F.C.S., and R.V. wrote the paper.

The authors declare no conflict of interest.

*This Direct Submission article had a prearranged editor.

Freely available online through the PNAS open access option.

[1]B.C. and A. Schraenen contributed equally to this work.

[2]B.N., F.C.S., and R.V. contributed equally to this work.

[3]To whom correspondence should be addressed. E-mail: rudi.vennekens@med.kuleuven.be.

This article contains supporting information online at www.pnas.org/cgi/content/full/0913107107/DCSupplemental.

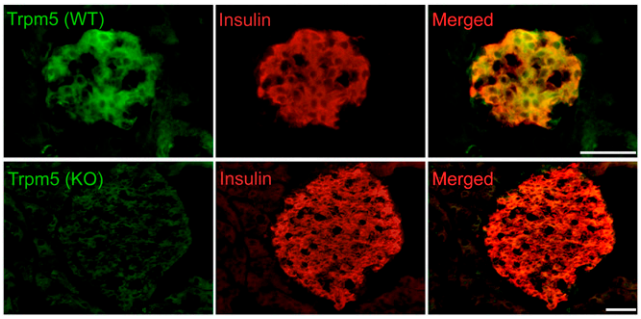

Fig. 1. Expression of TRPM5 protein in pancreatic islets of Langerhans immunostaining for TRPM5 and insulin of pancreatic islets from WT and *Trpm5*$^{-/-}$ mice.

determination of the time course of activation for this current, in relative isolation from other conductances in β-cells. In WT cells we found a time constant for activation ($\tau = 24.1 \pm 3.5$ ms; $n = 14$), which is similar to what has been shown before for TRPM5 (27). Furthermore, the Ca^{2+}-activated current in these conditions in WT cells showed a clear bell-shaped dependency on $[Ca^{2+}]_{cyt}$ (Fig. 2*F*), which corresponds to the Ca^{2+}-dependence of TRPM5 (13, 27). Obviously, the current in *Trpm5*$^{-/-}$ cells is strongly reduced at each $[Ca^{2+}]_{cyt}$ level (Fig. 2 *C* and *F*). Finally, the Ca^{2+}-activated current in WT cells displayed a cation conductance sequence $Li^+ > Na^+ >> Ca^{2+} \sim NMDG^+$, which is essentially the same as reported for TRPM5, but different from the background current in *Trpm5*$^{-/-}$ cells ($Na^+ > Li^+ >> Ca^{2+} \sim NMDG^+$). Thus, it is clear that TRPM5 is an important constituent of the calcium-activated cation current in pancreatic β-cells. Other presently known molecular candidates for this class of ion channels include TRPC5 (28, 29), TRPM2 (30), and TRPM4, which may constitute the remaining Ca^{2+}-activated cation current in *Trpm5*$^{-/-}$ β-cells. At least TRPM2 and TRPM4 are also expressed in insulin-secreting cell lines and in mouse pancreatic islets (31, 32). Notably, deletion of the *Trpm4* gene has no effect on glucose tolerance or on insulin release from pancreatic islets (33). Finally, note that the current described here is fundamentally different from the "leak" channel, NALCN, proposed recently in β-cells (34, 35).

Slower Intracellular Ca^{2+} Oscillations in Islets Derived from *Trpm5*$^{-/-}$ Mice. To find clues about the functional role of TRPM5 in pancreatic β-cells, we first turned to glucose-induced Ca^{2+} oscillations. β-Cells display very characteristic $[Ca^{2+}]_{cyt}$ oscillations in response to high glucose concentrations, which critically regulate the release of insulin. To analyze glucose-induced signaling in intact islets, we monitored $[Ca^{2+}]_{cyt}$ dynamics in intact Fura-2–loaded islets of WT and *Trpm5*$^{-/-}$ mice. The basal fura-2 fluorescence ratio (F_{350}/F_{380}), in a nonstimulatory glucose concentration (3 mM), was similar in WT and *Trpm5*$^{-/-}$ islets (WT, 1.16 ± 0.03; vs. *Trpm5*$^{-/-}$, 1.20 ± 0.02; $P = 0.16$; $n = 27$–33 from five to seven mice). Islets from both genotypes had a similar glucose concentration threshold for triggering $[Ca^{2+}]_{cyt}$ oscillations (WT, 6.20 ± 0.243; vs. *Trpm5*$^{-/-}$, 6.21 ± 0.239; $P = 0.97$; $n = 14$–15 from four to five mice), indicating that glucose metabolism preceding glucose-induced electrical activity is not changed in *Trpm5*$^{-/-}$ mice.

Increasing extracellular glucose concentration from 3 to 10 mM elicited an oscillatory increase in $[Ca^{2+}]_{cyt}$ in both WT and *Trpm5*$^{-/-}$

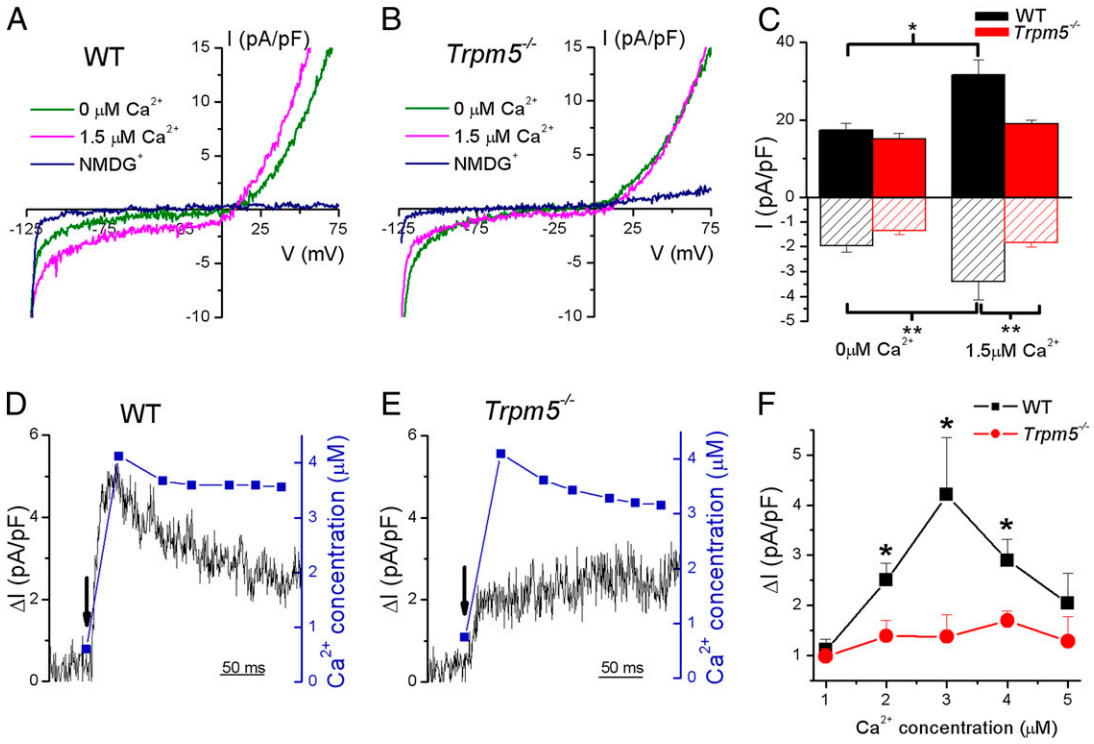

Fig. 2. Characterization of a TRPM5-dependent calcium-activated nonselective cation current in single pancreatic islet cells. (*A*) Representative current traces in response to voltage ramps from −125 mV to +125 mV in WT cells dialyzed with either 0 or 1.5 μM Ca^{2+} in a bath solution containing 150 mM Na^+ or 150 mM $NMDG^+$. (*B*) Representative current traces as in *A* in *Trpm5*$^{-/-}$ cells. (*C*) Mean current densities at +80 mV and −80 mV in WT and *Trpm5*$^{-/-}$ cells ($n = 12$–14) in response to 0 Ca or 1.5 μM Ca^{2+} as in *A*. (*D*) Representative example of a current measured in a WT cell in the whole cell configuration during a step at +80 mV showing the activation kinetics of the calcium-activated current. After 60 ms, flash photolysis of caged Ca^{2+} was performed (arrow). $[Ca^{2+}]_{cyt}$ was measured simultaneously. (*E*) Representative example of a current measured as in *D* in a *Trpm5*$^{-/-}$ cell. (*F*) Ca^{2+} dependency of the current activated after uncaging of Ca^{2+} at +80 mV in WT and *Trpm5*$^{-/-}$ cells. The response is the difference in current density before and after the flash photolysis and is obtained from experiments as shown in *D* and *E*. *$P < 0.05$.

islets (Fig. 3*A*). During a typical 20-min stimulation with 10 mM glucose, the average increase in $[Ca^{2+}]_{cyt}$, as evaluated from F_{350}/F_{380}, was not different between WT and *Trpm5*$^{-/-}$ islets (WT, 0.26 ± 0.03; vs. *Trpm5*$^{-/-}$, 0.21 ± 0.02; $P = 0.23$; $n = 28$–33 from five to seven mice; Fig. 3*B*). Strikingly, *Trpm5*$^{-/-}$ islets exhibited overall a significantly lower frequency of $[Ca^{2+}]_{cyt}$ oscillations (0.82 ± 0.11 peaks/min in WT; 0.38 ± 0.03 peaks/min in *Trpm5*$^{-/-}$ islets; $P = 0.00078$; $n = 28$–34 from five to seven mice; Fig. 3*C*).

However, in line with previous work (10, 36, 37), we observed significant variability in the oscillatory pattern among individual islets. Using Fourier analysis, three different oscillatory patterns could be distinguished in WT islets in 10 mM glucose (Fig. S2) (*i*): slow oscillators display relevant frequencies below 0.015 Hz (*ii*), fast oscillators display relevant frequencies above 0.015 Hz, and (*iii*) mixed (compound) oscillators display relevant frequencies in both slow and fast frequency regions (for a detailed description, see Fig. S2). In preparations from WT mice, the proportion of islets exhibiting slow (38.2%), mixed (38.2%), and fast (23.6%) $[Ca^{2+}]_{cyt}$ oscillations (Fig. 3*D*) was comparable to distributions reported before (10, 37). Remarkably, fast oscillating islets were completely lacking in preparations from *Trpm5*$^{-/-}$ mice, in which 89.3% of the islets were classified as slow oscillators and the remaining islets showed mixed oscillations (χ^2 analysis, $P = 0.0006$; Fig. 3*D*). An analogous difference is observed when islets were stimulated with a supramaximal concentration of glucose (20 mM). This leads to longer plateaus of increased Ca^{2+}, both in WT and KO islets. In WT islets, a sustained Ca^{2+} plateau is the most prevalent pattern, whereas Ca^{2+} oscillations during the stimulation period were observed in only a small subset of the islets. Strikingly, in *Trpm5*$^{-/-}$ islets, the oscillating pattern is the more prevalent (Fig. S3; χ^2 analysis, $P = 0.025$). Finally, it should be noted that increased glucose-induced $[Ca^{2+}]_{cyt}$ oscillation frequency in β-cells lacking the BETA3 subunit of voltage-gated Ca^{2+} channels can be accounted for by enhanced formation of inositol 1,4,5-trisphosphate and increased Ca^{2+} mobilization from intracellular stores in *Beta3*$^{-/-}$ islets (38). In *Trpm5*$^{-/-}$ islets, this pathway is not altered, as release of calcium from the intracellular stores was the same in WT and *Trpm5*$^{-/-}$ islets upon stimulation with acetylcholine [an activator of the phospholipase C pathway (39); Fig. S4], revealing no differences in the PI signaling pathway or the amount of Ca^{2+} in intracellular stores. Taken together, these data demonstrate that TRPM5 is specifically required for the generation of fast $[Ca^{2+}]_{cyt}$ oscillations upon high glucose stimulation.

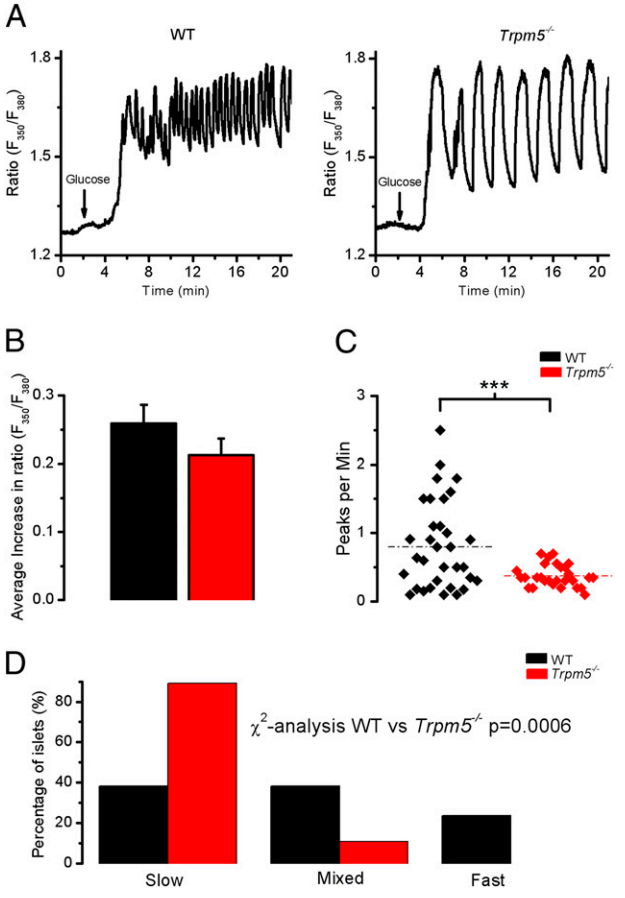

Fig. 3. Overall reduced frequency of intracellular Ca^{2+} oscillations in isolated islets from *Trpm5*$^{-/-}$ mice as a result of a lack of fast oscillations. (*A*) Effect of glucose (10 mM) on the $[Ca^{2+}]_{cyt}$ in islets from WT and *Trpm5*$^{-/-}$ mice. Initially, the islets were bathed in a solution containing 3 mM glucose. Arrows indicate application of 10 mM glucose. (*B*) Average increase in ratio (F_{350}/F_{380}) after stimulation with 10 mM glucose in islets from WT and *Trpm5*$^{-/-}$ mice ($n = 28$–34 from five to seven mice; $P = 0.23$). (*C*) Frequency of oscillations in individual experiments from WT and *Trpm5*$^{-/-}$ islets, counted as the number of peaks per min ($n = 28$–34 from five to seven mice). $[Ca^{2+}]_{cyt}$ increase of 15% was considered to be an oscillation, when 100% is the amplitude between the baseline and the highest level reached in 10 mM glucose. ***$P < 0.001$. (*D*) Proportion of islets showing slow, mixed, and fast oscillation patterns according to Fourier analysis in WT (38.2%, 38.2%, and 23.6%, respectively) and *Trpm5*$^{-/-}$ islets (89.3%, 10.7%, and 0%, respectively): $n =$ 28 to 34 from five to seven mice; χ^2 analysis WT vs. *Trpm5*$^{-/-}$: $P = 0.0006$.

Membrane Potential Oscillations from WT and *Trpm5*$^{-/-}$ Islets. As TRPM5 is a Ca^{2+}-activated, but Ca^{2+}-impermeable, cation channel, it can be anticipated that TRPM5 will influence $[Ca^{2+}]_{cyt}$ oscillations through an effect on membrane potential (V_m). Typically, glucose-stimulated pancreatic islets display depolarizing oscillations of membrane potential triggering bursts of action potentials (Fig. 4*A*). Oscillations in intracellular Ca^{2+} and V_m in glucose-stimulated islets are strictly coupled (Fig. S5*A*). Therefore, we performed combined V_m and $[Ca^{2+}]_{cyt}$ measurements, to unravel the role of TRPM5 in this process.

In line with the pattern of $[Ca^{2+}]_{cyt}$ oscillations, glucose-induced V_m oscillations in individual islets can be classified as slow (average frequency <0.015 Hz), fast (average frequency >0.015 Hz; Fig. 4*A*), or mixed, showing the typical pattern of clusters of V_m oscillations separated by prolonged silent intervals (40). In a group of WT islets ($n = 17$), the distribution of the different oscillation patterns was comparable to the distribution seen in $[Ca^{2+}]_{cyt}$ measurements (χ^2 analysis, $P = 0.09$): 47% of the islets were oscillating fast ($n = 8$), whereas 41.2% could be classified as slow oscillators ($n = 7$) and the remaining 11.8% ($n = 2$) showed compound oscillations. Likewise, *Trpm5*$^{-/-}$ islets ($n = 9$; χ^2 analysis, $P = 0.3$), only display slow oscillations. Thus, it is clear that the absence of fast $[Ca^{2+}]_{cyt}$ oscillations is mirrored by the absence of fast V_m oscillations in *Trpm5*$^{-/-}$ islets (Fig. 4*A*; χ^2 analysis, WT vs. *Trpm5*$^{-/-}$, $P = 0.019$).

To determine the contribution of TRPM5 to the bursting pattern in glucose-stimulated islets, we performed a detailed comparison of V_m changes in islets from both mouse strains. Detailed analysis of the individual action potentials on top of the depolarized plateau, revealed no significant differences between WT and *Trpm5*$^{-/-}$ islets concerning parameters like duration and maximal slope of the upstroke, duration of repolarization, and width at half-maximal amplitude. A tendency, although not statistically significant, toward reduced action potential amplitude was apparent in *Trpm5*$^{-/-}$ islets (Table S1 and Fig. S6). Slow burst oscillations were indistinguishable between WT and *Trpm5*$^{-/-}$ islets, with respect to the duration of the interburst interval, the slope of depolarization during the interburst interval, the threshold potential for burst initiation (Fig. 4*B*), the average burst duration, plateau fraction, resting potential, interburst potential, and the plateau potential (Table 1). As fast bursting is missing from *Trpm5*$^{-/-}$ mice, it seems evident that TRPM5 activity must be hidden in the difference between fast and slow bursting in WT islets. The most obvious differences in that comparison are burst

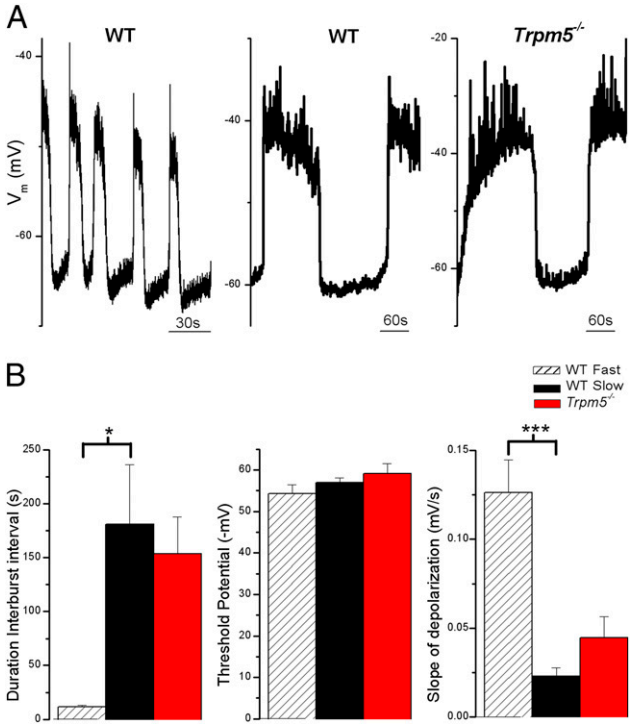

Fig. 4. V_m measurements in WT and *Trpm5*$^{-/-}$ islets stimulated with 10 mM glucose. (*A*) Representative examples of V_m measurements in WT islets showing fast (*Left*) and slow (*Middle*) oscillation patterns and in *Trpm5*$^{-/-}$ islets displaying slow oscillations (*Right*). (*B*) Comparison of duration of the interburst interval, threshold potential for burst initiation, and slope of the depolarization during the interburst interval in WT fast- and slow-oscillating islets and in *Trpm5*$^{-/-}$ slow-oscillating islets (n = 8–9 from five to six mice). *P < 0.05; ***P < 0.001.

duration, interburst interval, and maximal slope of the interburst interval. Burst duration is significantly shorter in fast oscillating islets compared with slow islets (Table 1). This is, however, unlikely to result from a lack of TRPM5 activity, as a Ca^{2+}-activated cation channel would be expected to prolong the burst duration. Furthermore, in agreement with the unchanged average $[Ca^{2+}]_{cyt}$ increase in *Trpm5*$^{-/-}$ islets, the plateau fraction is similar in all groups (Table 1). Fast oscillators display a significantly shorter interburst interval, resulting in higher burst frequency. In parallel, the maximal slope of the interburst interval is significantly increased in fast oscillating islets compared with slow islets. It is clear from combined $[Ca^{2+}]_{cyt}$ and V_m measurements that the Ca^{2+}-transient overlaps with the interburst interval (Fig. S5*A*), so it is likely that TRPM5 is active during the interburst interval. As the increased slope is lacking in *Trpm5*$^{-/-}$ islets, our data strongly suggest that TRPM5 is contributing to the depolarizing current during the interburst interval to drive the V_m toward the threshold for a new burst of activity.

Interestingly, a mathematical model of Ca^{2+} and V_m changes in a glucose-stimulated pancreatic β-cell reproduces this phenotype (Fig. S5*B*). In this model, removing a Ca^{2+}-activated monovalent cation conductance significantly reduces the oscillation frequency, as we observe in our KO mouse model. This is a result of the lack of a depolarizing current in the interburst interval, which shapes the slow depolarization of the membrane potential to reach the threshold for a new burst of activity (Fig. S5*C*). Note that the increased Ca^{2+} during the burst of activity overlaps to a large part with the interburst interval, as we also observe in simultaneous Ca^{2+} and V_m measurements (Fig. S5 *A* and *B*), explaining why TRPM5 would be active in this period.

It's important to mention here, however, that it is unclear what the exact mechanism behind the variability of the oscillation pattern of a pancreatic islet is (9), and why TRPM5 is apparently only functionally relevant in a (fast-oscillating) subpopulation of the islets. Several models for glucose-induced Ca^{2+} oscillations exist, of which the most successful propose a complex interplay among $[Ca^{2+}]_{cyt}$ levels, ion channel activity, glycolytic rate, and mitochondrial respiration (6). Bertram et al. (6) propose that slow oscillations (period between 2 and 7 min) represent oscillations in glycolytic activity and that fast oscillations (period as long as tens of seconds) are controlled by ion channel activity during persistent high glycolytic activity. Compound bursting would represent a complex interplay among several of the aforementioned factors. Our data fit well into this model, in a sense that we can show that TRPM5 is essential for the occurrence of fast but not slow oscillations and that also compound bursting is largely lacking in *Trpm5*$^{-/-}$ islets. An interesting hypothesis might be that the weight of TRPM5-mediated depolarization is coupled to the glycolytic rate in the cell. Thus, at a constantly high glycolytic rate, which is a necessity for fast oscillations according to Bertram et al. (6), TRPM5 activity would be able to depolarize V_m in the interburst interval, as the hyperpolarizing K_{ATP} current is largely inactive at that point. Conversely, during an oscillating glycolytic rate, TRPM5 would be inadequate to depolarize V_m during the low point of glycolytic activity, corresponding to the interburst interval between slow oscillations (6) as a result of high activity of K_{ATP}.

Table 1. Characteristics of V_m measurements in WT and *Trpm5*$^{-/-}$ islets during stimulation with 10 mM glucose

	WT			*P* value	
Characteristic	Slow (n = 7 from 5 mice)	Fast (n = 8 from 6 mice)	*Trpm5*$^{-/-}$:Slow (n = 9 from 5 mice)	WT: Slow vs. fast	Slow: WT vs. *Trpm5*$^{-/-}$
Duration of interburst interval, s	180.8 ± 55.4	11.8 ± 1.4	153.5 ± 34.0	0.013*	0.78
Slope of depolarization in the interburst interval, mV/s	0.023 ± 0.004	0.13 ± 0.02	0.034 ± 0.01	0.0001*	0.18
Threshold potential for burst initiation, mV	−56.9 ± 1.1	−54.3 ± 2.1	−59.1 ± 2.4	0.27	0.64
Average duration of burst plateau, s	120.5 ± 17.6	12.7 ± 3.5	114.7 ± 17.4	<0.0001*	0.82
Plateau fraction, %	0.47 ± 0.04	0.55 ± 0.06	0.6 ± 0.05	0.22	0.56
Plateau potential, mV	−42.2 ± 2.5	−49.2 ± 3.0	−46.2 ± 4.4	0.091	0.41
Interburst potential, mV	−61.2 ± 2.3	−59.4 ± 2.72	−66.7 ± 1.5	0.61	0.14
Resting potential, mV	−70.4 ± 0.8	−71.5 ± 1.0	−73.0 ± 2.1	0.12	0.98

Comparison of different parameters (in mean ± SEM) of V_m in WT slow (n = 7 from 5 mice) vs. WT fast (n = 8 from 6 mice) oscillating islets and WT slow vs. *Trpm5*$^{-/-}$ slow oscillating islets (n = 9 from 5 mice). The plateau fraction is calculated as the sum of burst lengths divided by the total period of glucose stimulation.
*Significant at P < 0.05.

Metabolic Phenotype of *Trpm5*$^{-/-}$ Mice. To determine whether the lack of fast oscillations has consequences for pancreatic islet function, glucose-induced insulin release from freshly isolated islets was measured. Insulin release was significantly reduced in *Trpm5*$^{-/-}$ islets when stimulated with 10 or 20 mM glucose (Fig. 5*A* and Fig. S5). Importantly, the insulin content of individual islets (WT, 65.9 ± 5.5 ng insulin/islet; vs. *Trpm5*$^{-/-}$, 57.2 ± 5.2 ng insulin/islet; $P = 0.27$; $n = 8$) and the pancreatic insulin content in *Trpm5*$^{-/-}$ islets (WT, 45.9 ± 6.6 μg insulin per pancreas; vs. *Trpm5*$^{-/-}$, 51 ± 6.8 μg insulin per pancreas; $P = 0.58$; and WT, 90.8 ± 12.7 μg insulin per g of pancreas; vs. *Trpm5*$^{-/-}$, 105.1 ± 1.3 μg insulin per g of pancreas; $P = 0.38$; $n = 3$) were unchanged, indicating that TRPM5 is not required for insulin synthesis or storage. β-Cells release insulin through Ca^{2+}-dependent exocytosis of membrane vesicles (41). Cell capacitance measurements from isolated β-cells reveal a similar exocytotic response to the Ca^{2+}-ionophore ionomycin (ΔC_m, 0.70 ± 0.26 pF in WT cells vs. 0.74 ± 0.18 pF in *Trpm5*$^{-/-}$ cells; $P = 0.77$; $n = 6$ per group), excluding a defect in Ca^{2+}-dependent exocytosis as a result of *Trpm5* gene deletion. Considering that the time-averaged $[Ca^{2+}]_{cyt}$ signal (and the plateau fraction in V_m measurements) upon glucose stimulation was not significantly different from WT, it may seem difficult to explain a significant reduction in Ca^{2+}-dependent insulin release. However, in this aspect, our results are fully consistent with previous work in β-cells (38) as well as in other secretory cell types such as pulmonary alveolar cells (42) and somatotropes (43), showing that fast Ca^{2+} oscillations are more efficient than slow oscillations in triggering exocytosis of secretory vesicles. It is clear that Ca^{2+} exhibits a strong cooperativity in triggering exocytosis from β-cells, suggesting that four to five Ca^{2+} ions bind to the exocytotic machinery to induce vesicle fusion (44). This nonlinearity may, at least partially, underlie the more efficient insulin release in rapidly oscillating islets. Moreover, oscillatory changes in $[Ca^{2+}]_{cyt}$ in β-cells were also shown to be much more efficient than sustained changes in mobilizing and/or priming vesicles for release (38).

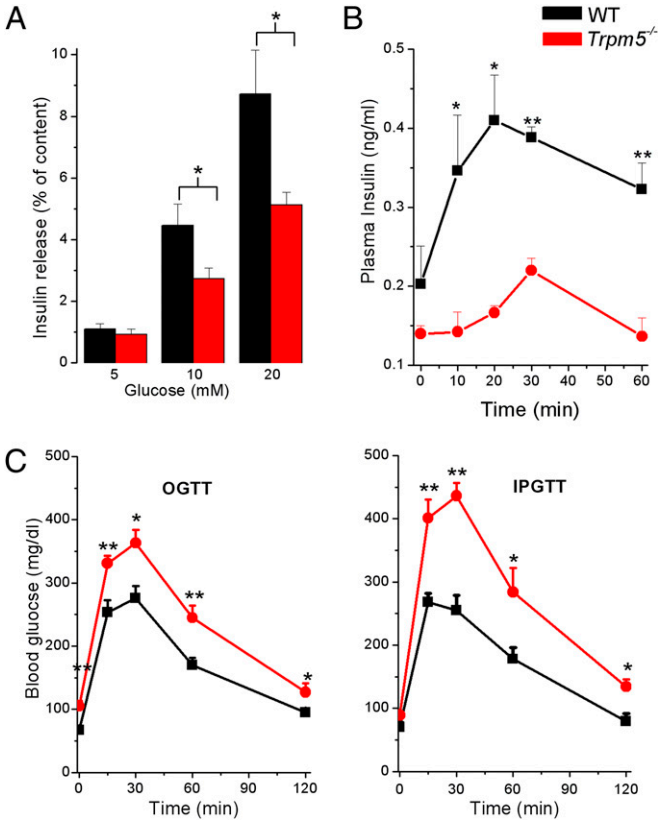

Fig. 5. Reduced glucose-induced insulin release leads to a disturbed glucose tolerance in *Trpm5*$^{-/-}$ mice. (*A*) Insulin secretion from WT and *Trpm5*$^{-/-}$ islets. Islets were challenged with different glucose concentrations as indicated ($n = 8$ per group). Insulin release was normalized to islet insulin content. *$P < 0.05$. (*B*) Plasma insulin levels after an i.p. glucose injection in overnight fasted WT and *Trpm5*$^{-/-}$ mice ($n = 4$–5 mice; *$P < 0.05$; **$P < 0.01$). (*C*) OGTT and IPGTT glucose tolerance tests in WT and *Trpm5*$^{-/-}$ mice. ($n = 7$ WT and $n = 7$ *Trpm5*$^{-/-}$ mice for OGTT, $n = 4$ WT and $n = 4$ *Trpm5*$^{-/-}$ mice for IPGTT. *$P < 0.05$; **$P < 0.01$.)

Finally, in conscious mice, overnight fasting blood glucose levels were significantly higher in *Trpm5*$^{-/-}$ mice (95 ± 3 mg/dL) versus WT mice (72 ± 2 mg/dL; $n = 25$–28; $P = 0.0009$). No changes were observed between both mouse lines in an insulin tolerance test (Fig. S7). However, in agreement with the reduced insulin release measured from isolated islets, plasma insulin levels after i.p. glucose injection in overnight fasted male mice were significantly reduced in *Trpm5*$^{-/-}$ mice compared with WT mice (Fig. 5*B*). As a consequence, results of oral glucose tolerance test (OGTT) and i.p. glucose tolerance test (IPGTT) show a reduced glucose tolerance in *Trpm5*$^{-/-}$ mice (Fig. 5*C*). These data convincingly show that reduced glucose-induced insulin release from β-cells leads to a moderate but significant glucose intolerance in *Trpm5*$^{-/-}$ mice.

Conclusion

We identified *Trpm5* as an important gene for the function of mouse pancreatic β-cells. Deletion of *Trpm5* results in an impaired glucose tolerance caused by a reduced glucose-induced insulin release from pancreatic islets. In this way, insight in pancreatic TRPM5 function could consolidate our understanding of the pathogenesis of type II diabetes and might provide a unique target for the treatment of this disease.

Materials and Methods

Experimental procedures are described in more detail in *SI Materials and Methods*.

Mice. *Trpm5*$^{-/-}$ mice (45) were backcrossed eight generations in the C57BL/6J background and WT C57BL/6J mice were used as controls. Only male mice were used for experiments. All animal experiments were carried out in accordance with the European Union Community Council guidelines and approved by the local ethics committee.

Preparation of Islets. Islets were isolated from male mice at 10 to 14 weeks of age via collagenase digestion as described previously (46).

Solutions. For whole-cell current measurements, pipette solution contained (in mM) 20 NaCl, 120 NaAsp, 10 Hepes. $MgCl_2$, $CaCl_2$, and the appropriate Ca^{2+} buffer were added according to the CaBuf program (*ftp://ftp.cc.kuleuven.ac.be/pub/droogmans/cabuf.zip*) to obtain 1 mM free Mg^{2+} and the desired free Ca^{2+}-concentration. Bath solution contained (in mM) 150 NaCl, 5 $MgCl_2$, 10 Hepes, and 10 glucose. Pipette solution for flash-uncaging contained (in mM) 20 CsCl, 120 CsAsp, 20 Hepes, 2 $CaCl_2$, 5 DMNP-EDTA [1-(4.5-dimethoxy-2-nitrophenyl)-EDTA, Molecular Probes], 1 Fura-2FF (Teflabs); and bath solution contained (in mM) 140 CsAsp, 5 $MgCl_2$, 10 Hepes, 10 glucose, 1 μM nifedipine (Sigma-Aldrich) and 100 nM tetrodotoxin (Sankyo). Standard extracellular solution for calcium imaging measurements contained (in mM): 120 NaCl, 4.8 KCl, 2.5 $CaCl_2$, 1.2 $MgCl_2$, 10 Hepes, pH 7.4, with NaOH, with different concentrations of glucose added as indicated. For V_m and combined measurements, bath solution contained (in mM): 138 NaCl, 5.6 KCl, 1.2 $MgCl_2$, 2.6 $CaCl_2$, 10 Hepes, pH 7.4, with NaOH; and pipette solution contained (in mM): 10 KCl, 10 NaCl, 70 K_2SO_4, 7 $MgCl_2$, 5 Hepes, pH 7.35, with KOH, 300 μg/mL nystatin (Sigma-Aldrich) (47).

Electrophysiology and Calcium Measurements. Whole cell currents were measured at 31 °C to 33 °C from cells with a capacitance >5 pF (WT, 6.6 ± 0.3 pF; vs. *Trpm5*$^{-/-}$, 6.9 ± 0.3 pF; $P = 0.42$; $n = 29$–37), being most likely β-cells (26). $[Ca^{2+}]_{cyt}$ was measured by monitoring the Fura-2FF fluorescence signal (F_{350}/F_{380}). Calibration of the fura signal was done as previously described (27). Ramp protocol consisted of a 400-ms ramp from −100 mV toward +100 mV (whole cell current measurements) applied at 1 Hz or from +100 mV toward −100 mV (calcium

uncaging), applied at 0.5 Hz (holding potential, 0 mV). Flash photolysis was performed after 60 ms during a 300-ms depolarizing step at +80 mV. $[Ca^{2+}]_{cyt}$ from Fura-2–loaded islets was measured monitoring fluorescence ratio (F_{350}/F_{380}) every second (after correction for background fluorescence) at 37 °C. V_m measurements were performed at 31 °C to 33 °C in the perforated patch configuration under current-clamp conditions. In combined measurements, V_m of a single cell within the islet and $[Ca^{2+}]_{cyt}$ of a region centered around the patch pipette were simultaneously monitored.

Glucose and Insulin Tolerance Tests. Glucose and insulin tolerance were analyzed in overnight-fasted and 6 h–fasted mice of 10–14 weeks age, respectively.

Insulin Release. Insulin release was measured from statically incubated, size-matched, freshly isolated islets using a commercially available ELISA kit (Mercodia).

Data Analysis. Origin software (version 7.0; OriginLab) was used for data analysis. Data are represented as mean ± SEM unless mentioned differently. Statistical analysis was performed with the Student *t* test unless mentioned differently. $P < 0.05$ was considered to represent a significant difference.

ACKNOWLEDGMENTS. We thank C. Zuker (University of California, San Diego) for providing the *Trpm5*$^{-/-}$ mice and Mikaela Granvik, Melissa Benoit, and Annelies Janssens for excellent technical assistance. This work was supported by a postdoctoral fellowship from the FWO Vlaanderen to K.L. and K.T.; research grants of the European Union (EURODIA FP6-518153), Belgian Ministry for Science Policy (Interuniversity Attraction Pole IUAP P6/40 and P6/28), Excellentiefinanciering EF/95/010, Research Foundation–Flanders (G.0172.03, 1.5.206.09 and G.0565.07), and Katholieke Universiteit Leuven (Geconcerteerde Onderzoeksacties GOA 2004/07, 2004/11, 2008/16); and by National Institutes of Health Grant DC03055 (to R.M. and Z.K.).

1. Ashcroft FM, Rorsman P (1989) Electrophysiology of the pancreatic beta-cell. *Prog Biophys Mol Biol* 54:87–143.
2. Hinke SA, Hellemans K, Schuit FC (2004) Plasticity of the beta cell insulin secretory competence: preparing the pancreatic beta cell for the next meal. *J Physiol* 558: 369–380.
3. MacDonald PE, Rorsman P (2006) Oscillations, intercellular coupling, and insulin secretion in pancreatic beta cells. *PLoS Biol* 4:e49.
4. Wiederkehr A, Wollheim CB (2008) Impact of mitochondrial calcium on the coupling of metabolism to insulin secretion in the pancreatic beta-cell. *Cell Calcium* 44:64–76.
5. Henquin JC, Meissner HP (1984) Significance of ionic fluxes and changes in membrane potential for stimulus-secretion coupling in pancreatic B-cells. *Experientia* 40: 1043–1052.
6. Bertram R, Sherman A, Satin LS (2007) Metabolic and electrical oscillations: partners in controlling pulsatile insulin secretion. *Am J Physiol Endocrinol Metab* 293:E890–E900.
7. Berggren PO, Larsson O (1994) Ca2+ and pancreatic B-cell function. *Biochem Soc Trans* 22:12–18.
8. Barker CJ, Leibiger IB, Leibiger B, Berggren PO (2002) Phosphorylated inositol compounds in beta -cell stimulus-response coupling. *Am J Physiol Endocrinol Metab* 283:E1113–E1122.
9. Nunemaker CS, et al. (2006) Glucose modulates [Ca2+]i oscillations in pancreatic islets via ionic and glycolytic mechanisms. *Biophys J* 91:2082–2096.
10. Liu YJ, Tengholm A, Grapengiesser E, Hellman B, Gylfe E (1998) Origin of slow and fast oscillations of Ca2+ in mouse pancreatic islets. *J Physiol* 508:471–481.
11. Nilius B, Owsianik G, Voets T, Peters JA (2007) Transient receptor potential cation channels in disease. *Physiol Rev* 87:165–217.
12. Nilius B, Voets T (2005) TRP channels: a TR(I)P through a world of multifunctional cation channels. *Pflugers Arch* 451:1–10.
13. Prawitt D, et al. (2003) TRPM5 is a transient Ca2+-activated cation channel responding to rapid changes in [Ca2+]i. *Proc Natl Acad Sci U S A* 100:15166–15171.
14. Hofmann T, Chubanov V, Gudermann T, Montell C (2003) TRPM5 is a voltage-modulated and Ca(2+)-activated monovalent selective cation channel. *Curr Biol* 13: 1153–1158.
15. Launay P, et al. (2002) TRPM4 is a Ca2+-activated nonselective cation channel mediating cell membrane depolarization. *Cell* 109:397–407.
16. Nilius B, et al. (2003) Voltage dependence of the Ca2+-activated cation channel TRPM4. *J Biol Chem* 278:30813–30820.
17. Fonfria E, et al. (2006) Tissue distribution profiles of the human TRPM cation channel family. *J Recept Signal Transduct Res* 26:159–178.
18. Prawitt D, et al. (2000) Identification and characterization of MTR1, a novel gene with homology to melastatin (MLSN1) and the trp gene family located in the BWS-WT2 critical region on chromosome 11p15.5 and showing allele-specific expression. *Hum Mol Genet* 9:203–216.
19. Kaske S, et al. (2007) TRPM5, a taste-signaling transient receptor potential ion-channel, is a ubiquitous signaling component in chemosensory cells. *BMC Neurosci* 8:49.
20. Kokrashvili Z, et al. (2009) Release of endogenous opioids from duodenal enteroendocrine cells requires Trpm5. *Gastroenterology* 137:598–606.
21. Enklaar T, et al. (2000) Mtr1, a novel biallelically expressed gene in the center of the mouse distal chromosome 7 imprinting cluster, is a member of the Trp gene family. *Genomics* 67:179–187.
22. Pérez CA, et al. (2002) A transient receptor potential channel expressed in taste receptor cells. *Nat Neurosci* 5:1169–1176.
23. Roe MW, et al. (1998) Characterization of a Ca2+ release-activated nonselective cation current regulating membrane potential and [Ca2+]i oscillations in transgenically derived beta-cells. *J Biol Chem* 273:10402–10410.
24. Leech CA, Habener JF (1998) A role for Ca2+-sensitive nonselective cation channels in regulating the membrane potential of pancreatic beta-cells. *Diabetes* 47:1066–1073.
25. Sturgess NC, Hales CN, Ashford ML (1987) Calcium and ATP regulate the activity of a non-selective cation channel in a rat insulinoma cell line. *Pflugers Arch* 409:607–615.
26. Barg S, Galvanovskis J, Göpel SO, Rorsman P, Eliasson L (2000) Tight coupling between electrical activity and exocytosis in mouse glucagon-secreting alpha-cells. *Diabetes* 49: 1500–1510.
27. Ullrich ND, et al. (2005) Comparison of functional properties of the Ca2+-activated cation channels TRPM4 and TRPM5 from mice. *Cell Calcium* 37:267–278.
28. Blair NT, Kaczmarek JS, Clapham DE (2009) Intracellular calcium strongly potentiates agonist-activated TRPC5 channels. *J Gen Physiol* 133:525–546.
29. Gross SA, et al. (2009) TRPC5 is a Ca2+ -activated channel functionally coupled to Ca2+ -selective ion channels. *J Biol Chem* 284:34423–34432.
30. Du J, Xie J, Yue L (2009) Intracellular calcium activates TRPM2 and its alternative spliced isoforms. *Proc Natl Acad Sci USA* 106:7239–7244.
31. Lange I, et al. (2009) TRPM2 functions as a lysosomal Ca2+-release channel in beta cells. *Sci Signal* 2:ra23.
32. Cheng H, et al. (2007) TRPM4 controls insulin secretion in pancreatic beta-cells. *Cell Calcium* 41:51–61.
33. Vennekens R, et al. (2007) Increased IgE-dependent mast cell activation and anaphylactic responses in mice lacking the calcium-activated nonselective cation channel TRPM4. *Nat Immunol* 8:312–320.
34. Swayne LA, et al. (2009) The NALCN ion channel is activated by M3 muscarinic receptors in a pancreatic beta-cell line. *EMBO Rep* 10:873–880.
35. Gilon P, Rorsman P (2009) NALCN: a regulated leak channel. *EMBO Rep* 10:963–964.
36. Gilon P, Shepherd RM, Henquin JC (1993) Oscillations of secretion driven by oscillations of cytoplasmic Ca2+ as evidences in single pancreatic islets. *J Biol Chem* 268:22265–22268.
37. Bergsten P, Grapengiesser E, Gylfe E, Tengholm A, Hellman B (1994) Synchronous oscillations of cytoplasmic Ca2+ and insulin release in glucose-stimulated pancreatic islets. *J Biol Chem* 269:8749–8753.
38. Berggren PO, et al. (2004) Removal of Ca2+ channel beta3 subunit enhances Ca2+ oscillation frequency and insulin exocytosis. *Cell* 119:273–284.
39. Winzell MS, Ahrén B (2007) G-protein-coupled receptors and islet function-implications for treatment of type 2 diabetes. *Pharmacol Ther* 116:437–448.
40. Beauvois MC, et al. (2006) Glucose-induced mixed [Ca2+]c oscillations in mouse beta-cells are controlled by the membrane potential and the SERCA3 Ca2+-ATPase of the endoplasmic reticulum. *Am J Physiol Cell Physiol* 290:C1503–C1511.
41. Rorsman P, et al. (2000) The Cell Physiology of Biphasic Insulin Secretion. *News Physiol Sci* 15:72–77.
42. Ashino Y, Ying X, Dobbs LG, Bhattacharya J (2000) [Ca(2+)](i) oscillations regulate type II cell exocytosis in the pulmonary alveolus. *Am J Physiol Lung Cell Mol Physiol* 279:L5–L13.
43. Holl RW, et al. (1988) Spontaneous oscillations of intracellular calcium and growth hormone secretion. *J Biol Chem* 263:9682–9685.
44. Eliasson L, et al. (2008) Novel aspects of the molecular mechanisms controlling insulin secretion. *J Physiol* 586:3313–3324.
45. Zhang Y, et al. (2003) Coding of sweet, bitter, and umami tastes: different receptor cells sharing similar signaling pathways. *Cell* 112:293–301.
46. Van Lommel L, et al. (2006) Probe-independent and direct quantification of insulin mRNA and growth hormone mRNA in enriched cell preparations. *Diabetes* 55: 3214–3220.
47. Smith PA, Ashcroft FM, Rorsman P (1990) Simultaneous recordings of glucose dependent electrical activity and ATP-regulated K(+)-currents in isolated mouse pancreatic beta-cells. *FEBS Lett* 261:187–190.